

# Yellowstone National Park whitebark pine planting water balance analysis

## Version 2.0

Stephen Huysman\*

July 2, 2025

## 1 Executive Summary

Broad-scale macroclimate (1 km) projections show the four planting sites selected in Yellowstone National Park (Avalanche Peak, Cub Creek, Chittenden (a), and Chittenden (b)) potentially transitioning to climates that are unlikely to be favorable for whitebark pine. However, despite end-of-century (2075–2099) projections that reveal the potential for extreme drought stress at all three locations, topoedaphic features that could potentially shelter planted tree seedlings from drought stress are identified as potential microrefugia based on modeled water balance at microclimate scales (1 m). Chittenden (a) shows the most extreme projected drought stress across the planting site, while larger areas of milder climate are projected to persist in the Chittenden (b), Avalanche Peak, and Cub Creek locations. An algorithm to select planting sites by maximizing projected Actual Evapotranspiration (a measure reflecting growing conditions favorable to plants) and minimizing projected Climatic Water Deficit (a measure of drought stress) across the three planting units selected planting locations in Chittenden (b) followed by Cub Creek, and Avalanche Peak, with no area selected in Chittenden (a). Chittenden (b) shows the lowest projected climatic water deficit out of all sites but low projected actual evapotranspiration at the location may lead to slower plant establishment and growth. Potential planting locations that seek to minimize drought stress under the most extreme climate projections while maintaining growing conditions favorable for plants include the northeastern hillslope in Chittenden (b), upper elevations in the eastern section of Avalanche Peak and the northwest facing hillside in Cub Creek. The central depression in Chittenden (a) shows the most favorable modeled water balance in the location; however, Chittenden (a) shows higher drought stress under all projections relative to the other planting locations.

## 2 Introduction

The suitability of planting sites in Yellowstone National Park that were selected for planting and seeding of whitebark pine (WBP; *Pinus albicaulis* Engelm.) in 2025 is assessed using a water balance model. First, the broad-scale macroclimatic suitability of the sites is assessed using a 1 km water balance model ([Tercek et al. 2021](#)) by comparing the historical and projected water balance of the planting sites to the climate found at other locations where whitebark pine is found across the contiguous United States (CONUS). Then, a high-resolution 1 m water balance model based on USGS LiDAR data is used to assess the suitability of planting sites selected in Yellowstone National Park by accounting for the influence of fine-scale topoedaphic features (slope, aspect, soil water holding capacity) on microclimate. Such fine-scale topoedaphic features have been shown to create significant variability in climates revealed by modeled local water balance, variability which may not be apparent when using coarser climate or terrain models ([Dyer](#)

---

\*shuysman@gmail.com

2019). These microclimates may allow for the persistence of climatically sensitive species such as whitebark pine, even when regional macroclimates are unfavorable, through the creation of climatic microrefugia which are locally favorable climates (Dobrowski 2011).

Here, the biophysical environment of plants is characterized by Actual Evapotranspiration (AET)—a measure of plant water use and favorable growing conditions—and Climatic Water Deficit (CWD)—a measure of drought stress. As indicators of plant water use (AET) and plant water need (CWD), these two variables are more robust predictors of vegetation distributions than other climate variables such as temperature or precipitation and are well correlated with vegetation distributions across local to continental spatial scales (Stephenson 1998). AET is directly correlated with growth rates in WBP seedlings and selecting planting sites with high AET can promote establishment (Laufenberg et al. 2020). Although no evidence of mortality caused by CWD has been observed in WBP, it is likely that high summer CWD could be detrimental to WBP establishment.

### 3 Planting site macroclimate

Planting suitability was evaluated at a macroclimate (1 km) scale to compare these sites to other regions where WBP grows. Historical (2000–2019) and ensemble end-of-century (2070–2099) RCP4.5 and RCP8.5 averages of annual AET and CWD were retrieved from the NPS 1 km Gridded Water Balance Model (Tercek, Gross, and Thoma 2023; Tercek et al. 2021) for WBP monitoring points located in the contiguous United States (CONUS) sourced from the white pine blister rust monitoring dataset (Huysman et al., in prep). WBP monitoring data located in Canada were excluded because they are not covered by the 1 km NPS Gridded Water Balance Model. The data were used to plot the current and projected climate of the planting sites analyzed in this report and other known locations of whitebark pine in a two-dimensional climate space characterized by the relationship between AET and CWD.

Using CONUS-wide WBP data to define the species' bioclimatic niche, macroclimate projections show all three planting units transitioning to the edge or outside of the historical climate conditions observed for WBP, particularly those within the Greater Yellowstone Ecosystem (GYE) (Figure 1). Chittenden (a) shows the most extreme projected climate at this scale, with highest AET and CWD out of all three units by 2070–2099 for both RCP4.5 and RCP8.5 ensemble projections. Chittenden (b) projections at this scale are similar to those of Chittenden (a), but slightly less extreme.

### 4 Planting site microclimate

Figures 2 and 3 show the microclimatic variability in average annual AET and CWD for historical and projected climate scenarios for the three planting units. The 1988 drought-year, where record low precipitation resulted in widespread drought and wildfire across the Greater Yellowstone Ecosystem (Christensen et al. 1989), shows much lower annual AET and much higher CWD for all three planting units compared to the 2004–2024 historical baseline average annual values.

Four projected climate scenarios (combinations of General Circulation models [GCM] and Representative Concentration Pathways [RCP]) were chosen to bracket extremes of changes in annual temperature and precipitation in Yellowstone National Park (Lawrence et al. 2021): *warm-wet* (MRI-CGCM3/RCP8.5), *warm-dry* (MRI-CGCM3/RCP4.5), *hot-dry* (HadGEM2-CC365/RCP8.5), and *hot-wet* (CanESM2/RCP8.5). All of these projections show increases in average annual AET and CWD compared to the 2004–2024 historical baseline. Three of the four projected scenarios show average annual CWD that are similar or greater in magnitude to the annual CWD experienced during 1988. These projections show that AET is not likely to be limiting at these sites but there is potential for extreme drought stress at all sites. Chittenden (a) shows the highest potential for drought stress, with the highest projected CWD under the *hot-dry* scenario.

Given this potential for drought stress at all planting units, the scenario with the highest projected CWD, *hot-dry*, will be used to represent the “worst-case” climate scenario, while *warm-dry* will represent the “best-case” climate scenario because it shows the lowest increases in projected CWD.

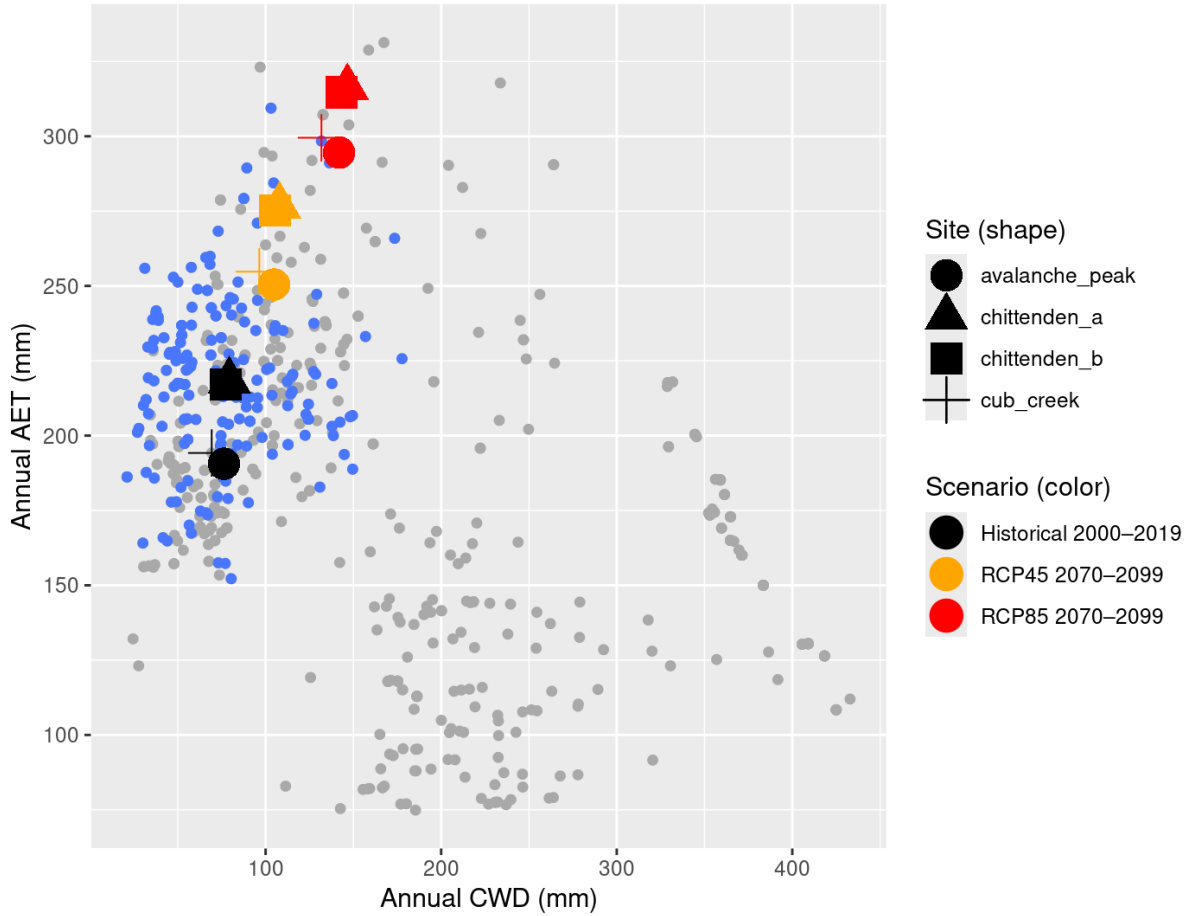


Figure 1: Macroclimate space of YELL whitebark pine at 1 km scale. Whitebark pine observations in CONUS from the white pine blister rust monitoring dataset (Huysman *et al.*, in prep) were used to create a bioclimatic niche of the species from historical (2000–2019) average annual AET and CWD from the NPS 1 km gridded water balance model (Tercek *et al.* 2021). Historical 2000–2019 average annual AET and CWD for points located in the Greater Yellowstone Ecosystem are highlighted in blue and all other WBP locations in the monitoring dataset across CONUS are grey. The three planting units in Yellowstone National Park analyzed in this report are shown as circles (Avalanche Peak), triangles (Chittenden [a]), squares (Chittenden [b]), and crosses (Cub Creek). Historical 2000–2019 water balance for these planting sites are shown in black and projected 2070–2099 water balance for the three planting units are shown in orange (RCP4.5) and red (RCP8.5).

## 5 Modeled 1 m water balance at planting sites

Modeled 1 m water balance for these planting sites shows significant variability in microclimates created by local terrain features. Figures 4, 5, 6, and 7 show the modeled 1 m water balance for historical and projected climate scenarios for Avalanche Peak, Cub Creek, Chittenden (a), and Chittenden (b), respectively. Spatial patterns of AET and CWD are consistent across time periods: more northern exposures and higher soil water holding capacities maximize AET and minimize CWD and more southern exposures and lower soil water holding capacities minimize AET and maximize CWD.

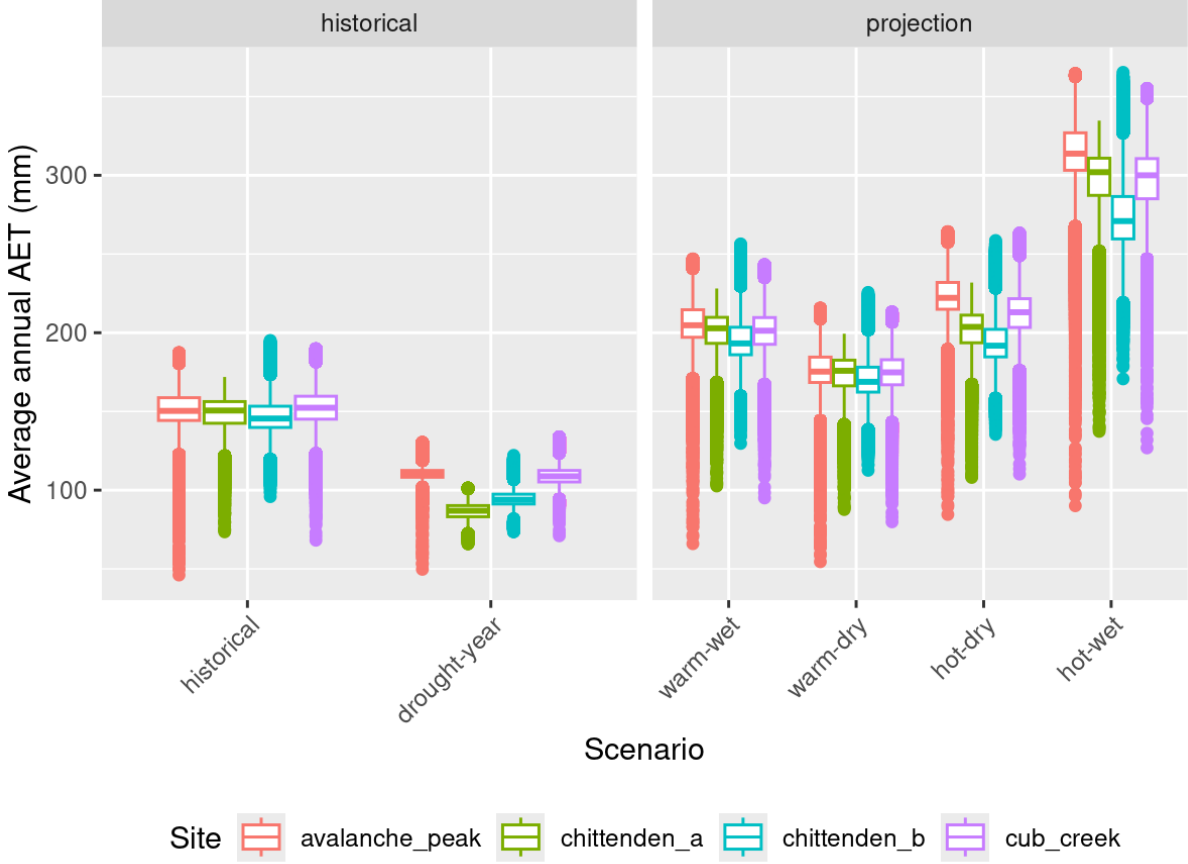


Figure 2: Microclimatic variability in annual AET across historical and projected climate scenarios. Modeled 1 m AET for two historical scenarios is shown: *historical* 2004-2024 historical average and *drought-year* 1988 annual AET. The average 2075-2099 average annual AET for four projections bracketing extremes of changes in annual temperature and precipitation are shown: *warm-wet* (MRI-CGCM3/RCP8.5), *warm-dry* (MRI-CGCM3/RCP4.5), *hot-dry* (HadGEM2-CC365/RCP8.5), and *hot-wet* (CanESM2/RCP8.5).

## 6 Planting site selection

Algorithmically selected planting locations that maximize AET and minimize CWD in end-of-century (2075–2099) projections are shown for the worst-case (hot-dry) (Figure 8) and best-case (warm-dry) (Figure 9) climate scenarios. The worst-case planting sites are conservative recommendations, that seek to minimize drought stress under the projection with highest CWD values (Figure 3). No planting locations are recommended by the algorithm in the Chittenden (a) location in either scenario because of its high projected CWD. Under the best-case climate scenario, minimizing drought stress is less critical because the projected drought stress is similar in magnitude to current conditions. However, the planting recommendations under the best-case scenario still seek to optimize conditions of water availability and drought stress.

These selected planting locations highlight specific areas that optimize growing conditions across the modeled microclimates found the planting units (Figures 8 and 9). Chittenden (b) has the lowest modeled projected CWD (Figure 3) and the northeast corner of the unit would allow planters to utilize the moderate projections of CWD here while maximizing AET to promote faster plant establishment and growth. Likewise, the eastern portion of Avalanche Peak and the northwest facing hillslope of Cub Creek provide a similarly optimal balance of AET and CWD. Chittenden (a) has a less favorable balance of AET and CWD across the planting location, however a portfolio approach to planting (Cho et al. 2025) would encourage planting some trees here, though perhaps less than the other locations, as a way to diversify risk and provide

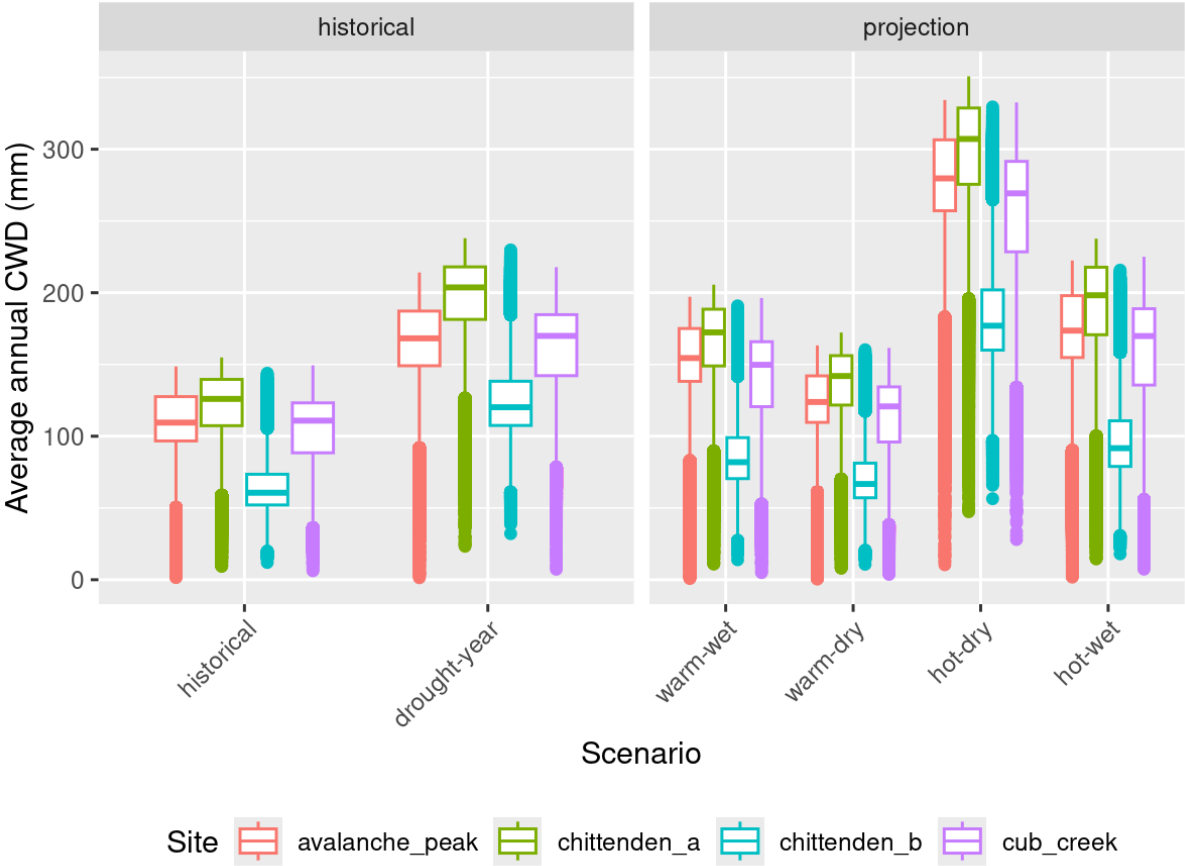


Figure 3: Microclimatic variability in annual Climatic Water Deficit (CWD) across historical and projected climate scenarios. Modeled 1 m CWD for two historical scenarios is shown: *historical* 2004-2024 historical average and *drought-year* 1988 annual CWD. The average 2075-2099 average annual CWD for four projections bracketing extremes of changes in annual temperature and precipitation are shown: *warm-wet* (MRI-CGCM3/RCP8.5), *warm-dry* (MRI-CGCM3/RCP4.5), *hot-dry* (HadGEM2-CC365/RCP8.5), and *hot-wet* (CanESM2/RCP8.5).

a hedge against the uncertainty in the range of climates that are projected.

The planting site recommendation algorithm works by selecting the 1,000,000 cells with highest AET and 1,000,000 cells with lowest CWD, then taking the union of those locations. Because there are locations with high AET that do not have low CWD, and vice-versa, the final area identified is smaller than the initial 1,000,000 cells. For the worst-case scenario, the final identified area is approximately  $0.08 \text{ km}^2$  and for the best-case scenario is approximately  $0.09 \text{ km}^2$ . The area selected in the best-case scenario is smaller because there is less overlap between pixels with high AET and low CWD in this scenario. This algorithm can be tweaked by increasing or decreasing the amount of cells to maximize AET/minimize CWD based on planting objectives and management risk objectives. For example, if more seed stock is available, the search area can be increased to find more suitable planting locations, at the cost of less optimal AET and CWD for some locations in the final union.

The planting sites selected by this algorithm are recommendations but should not be taken as absolute prescriptions. Planting decisions made using this data should consider observed soil characteristics in the field in conjunction with data presented here. This work examines the variability of microclimates within relatively coarse climate grid cells due to sub-grid cell topographic and edaphic features. These methods likely present a more accurate representation of climate at fine scales relevant to tree planting compared with unmodified use of gridded climate data products. However, several caveats and limitations exist with

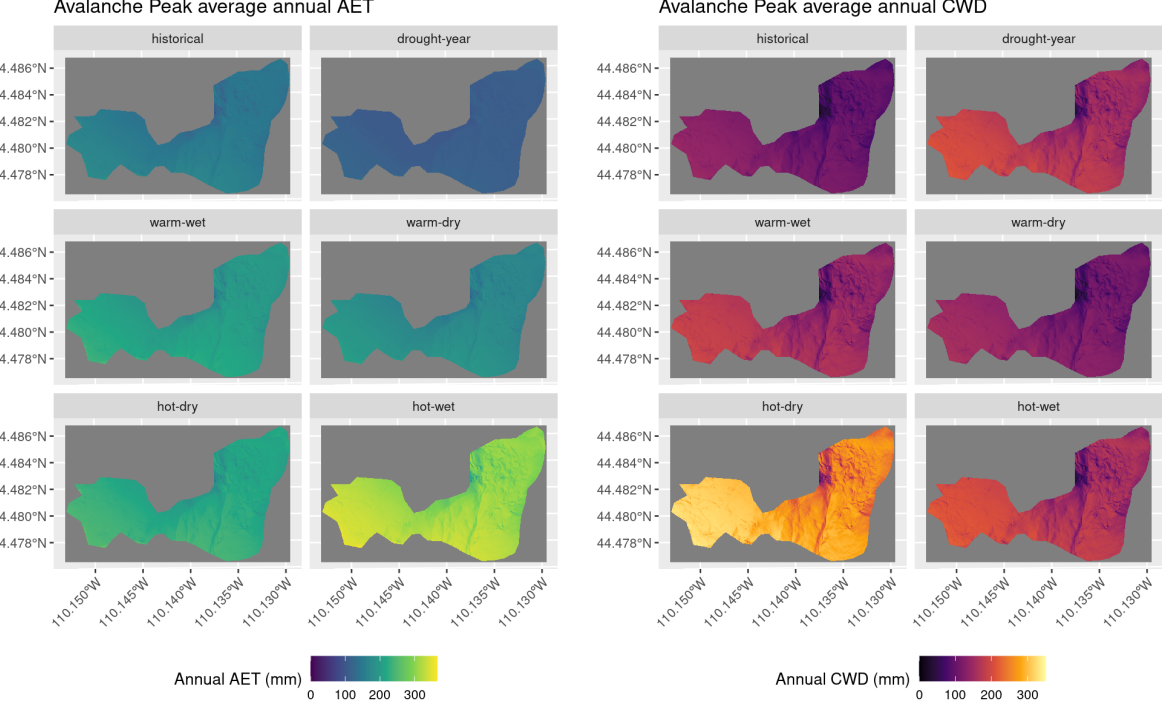


Figure 4: Modeled historical and projected average annual AET and CWD for Avalanche Peak. The color ramps used for AET and CWD visualizations are kept the same between planting units and climate scenarios to facilitate direct comparisons between units or time periods.

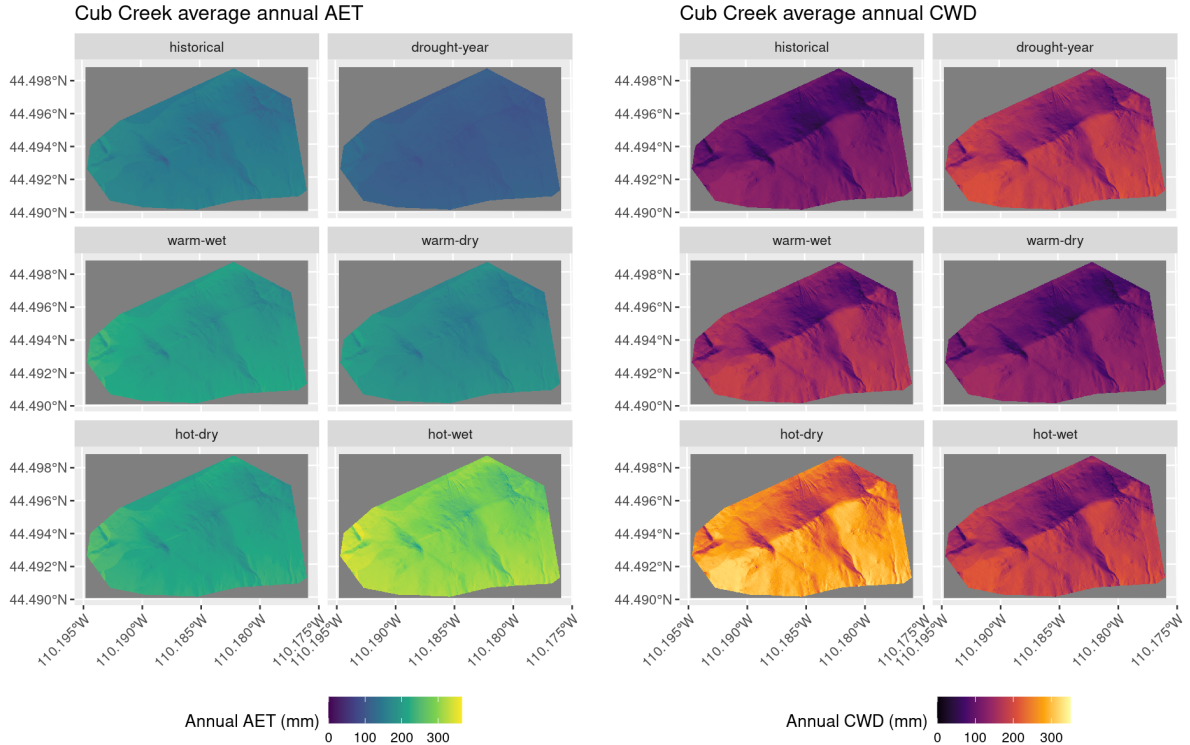


Figure 5: Modeled historical and projected average annual AET and CWD for Cub Creek. The color ramps used for AET and CWD visualizations are kept the same between planting units and climate scenarios to facilitate direct comparisons between units or time periods.

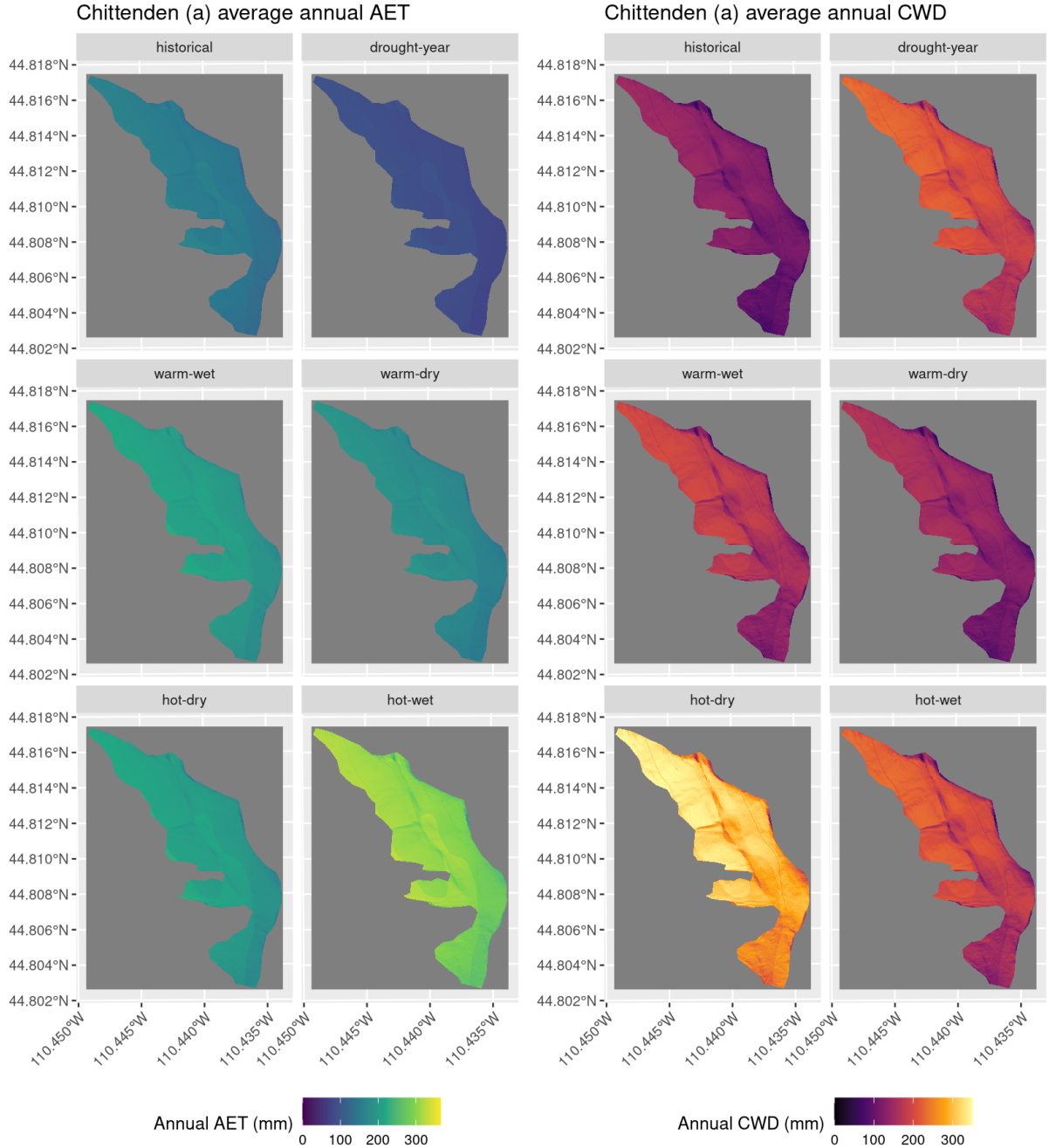


Figure 6: Modeled historical and projected average annual AET and CWD for Chittenden (a). The color ramps used for AET and CWD visualizations are kept the same between planting units and climate scenarios to facilitate direct comparisons between units or time periods.

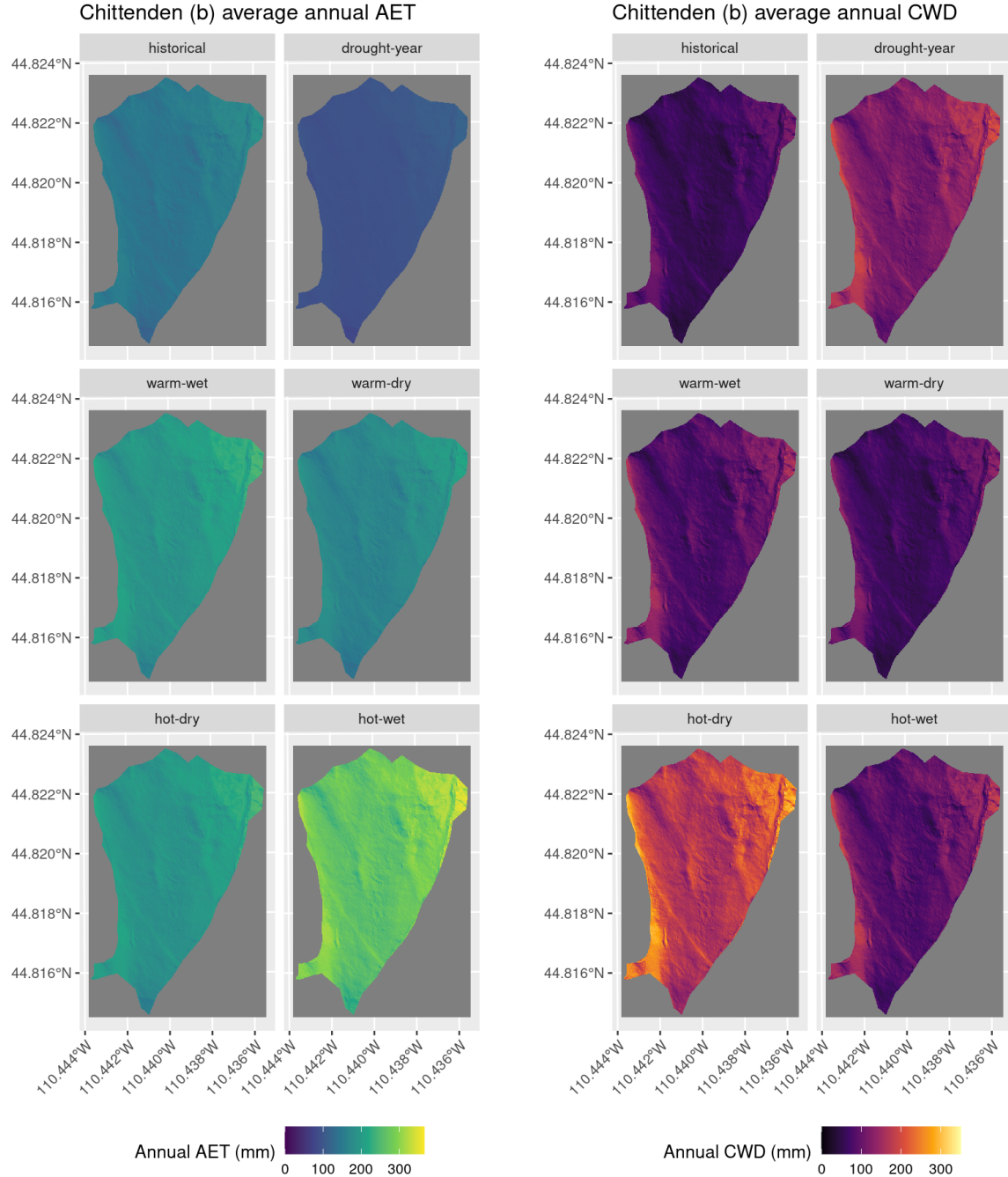


Figure 7: Modeled historical and projected average annual AET and CWD for Chittenden (b). The color ramps used for AET and CWD visualizations are kept the same between planting units and climate scenarios to facilitate direct comparisons between units or time periods.

the use of these methods.

Climate data from a single gridMET/MACA grid cell were used to represent each planting site analyzed in this report. These products are designed to show broad-scale patterns at regional scales that hold across large groups of pixels ([Abatzoglou 2013](#)). Uncertainty increases when these climate data products are applied to sub-grid cell scale locations such as point-scale data or the relatively small area examined here.

Temperature and precipitation data are not available at high resolutions in this study system and all available gridded climate data products have uncertainty in areas of complex topography such as mountainous regions ([Behnke et al. 2016](#)). The model and its climate inputs do not consider some sub-grid cell phenomena affecting air temperature such as temperature inversions and cold air drainage. Precipitation also varies at sub-grid cell scales due to topographic effects such as orographic precipitation ([Lin et al. 2001](#)). Snow accumulation and melt were modeled at the scale of the entire site, and not downscaled based on topography. In reality, snow accumulation and melt is affected by factors such as slope, aspect, as well as horizontal movement through snow drift ([Dingman 2015](#)).

The strength of this approach lies in its ability to detect relative differences in wetness and dryness across a landscape in a way that directly reflects the growing environment of plants. These relative patterns in the water balance across the landscape come with a higher degree of certainty than absolute estimates of AET and CWD. The model can help identify microclimates in locations where ideal combinations of soil and topography exist relative to other positions on the landscape. These locations may be difficult to identify visually, even for trained and experienced observers. For example, two hillslopes may have similar slope and aspect but different soil water holding capacities that lead to drier conditions on one than the other. In addition, planters may be skillful at identifying suitable planting sites based on current climatic conditions, but the methodology can quantify the potential change in a landscape position under plausible future climates relative to current conditions. The model reveals the potential for extreme drought stress in some landscape positions based on future climates, relative to current and past climatic conditions at the site. Therefore, planting site selection based on current conditions alone is unlikely to result in plantings that avoid this stress in the future.

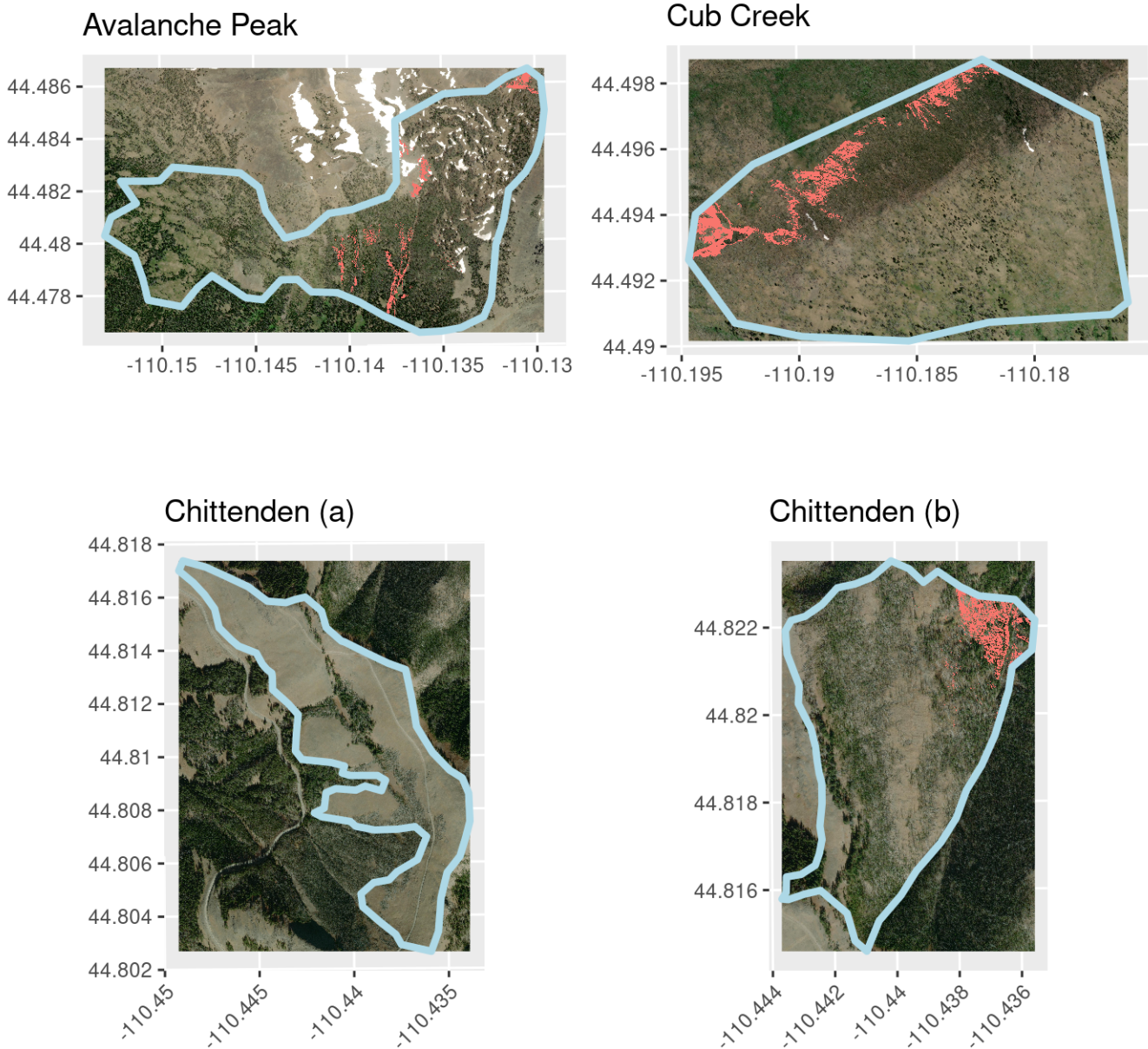


Figure 8: Algorithmically selected planting locations (highlighted in pink) for the *hot-dry* (worst-case) climate scenario. These are conservative planting location recommendations that seek to provide shelter from the most extreme projected drought conditions while maintaining conditions promoting plant growth. The final selected area is approximately  $0.08 \text{ km}^2$ . Note that no locations in Chittenden (a) were identified in this scenario. Tiles © Esri - Source: Esri, i-cubed, USDA, USGS, AEX, GeoEye, Getmapping, Aerogrid, IGN, IGP, UPR-EGP, and the GIS User Community.

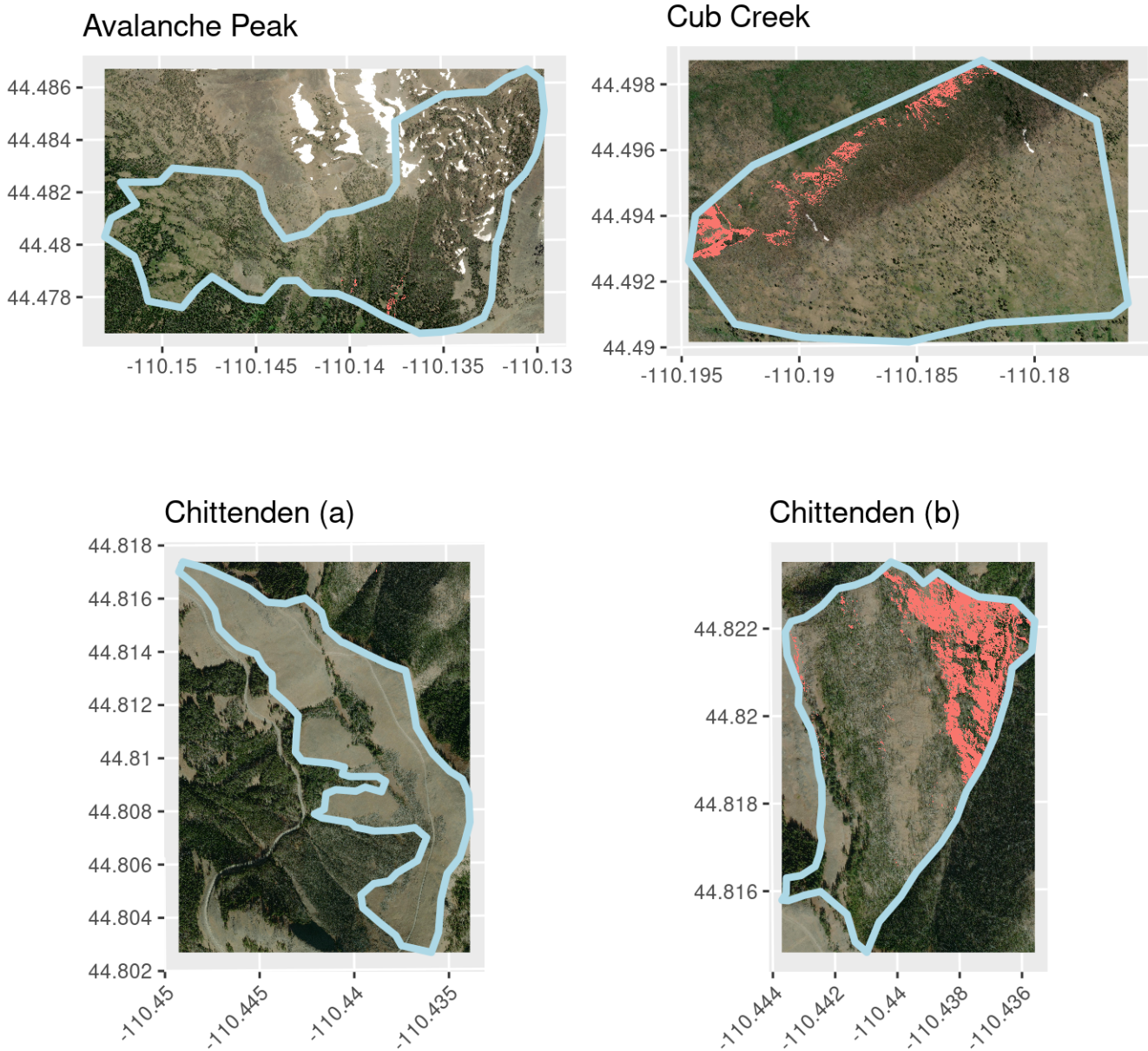


Figure 9: Algorithmically selected planting locations (highlighted in pink) for the *warm-dry* (best-case) climate scenario. There is only a slight increase in average CWD (drought stress) projected in this scenario, so avoidance of drought stress is less critical. These recommendations seek to optimize the balance of drought stress and water availability to promote plant growth and survival. Note that no locations in Chittenden (a) were identified in this scenario. The final selected area is approximately  $0.09 \text{ km}^2$ . Tiles © Esri - Source: Esri, i-cubed, USDA, USGS, AEX, GeoEye, Getmapping, Aerogrid, IGN, IGP, UPR-EGP, and the GIS User Community.

## 7 Acknowledgments

Funding for this work was provided by the Northern Rockies Conservation Cooperative.

Computational efforts were performed on the Tempest High Performance Computing System, operated and supported by University Information Technology Research Cyberinfrastructure (RRID:SCR\026229) at Montana State University.

## 8 References Cited

- Abatzoglou, John T. 2013. "Development of Gridded Surface Meteorological Data for Ecological Applications and Modelling." *International Journal of Climatology* 33 (1): 121–31. <https://doi.org/10.1002/joc.3413>.
- Behnke, R., S. Vavrus, A. Allstadt, T. Albright, W. E. Thogmartin, and V. C. Radeloff. 2016. "Evaluation of Downscaled, Gridded Climate Data for the Conterminous United States." *Ecological Applications* 26 (5): 1338–51. <https://www.jstor.org/stable/24818120>.
- Cho, Frankie H. T., Paolo Aglonucci, Ian J. Bateman, Christopher F. Lee, Andrew Lovett, Mattia C. Mancini, Chrysanthi Rapti, and Brett H. Day. 2025. "Resilient Tree-Planting Strategies for Carbon Dioxide Removal under Compounding Climate and Economic Uncertainties." *Proceedings of the National Academy of Sciences* 122 (10): e2320961122. <https://doi.org/10.1073/pnas.2320961122>.
- Christensen, Norman L., James K. Agee, Peter F. Brussard, Jay Hughes, Dennis H. Knight, G. Wayne Minshall, James M. Peek, et al. 1989. "Interpreting the Yellowstone Fires of 1988." *Bioscience* 39 (10): 678–85. <https://doi.org/10.2307/1310998>.
- Dingman, S. Lawrence. 2015. *Physical Hydrology*. Third. Long Grove, Illinois: Waveland Press, Inc.
- Dobrowski, Solomon Z. 2011. "A Climatic Basis for Microrefugia: The Influence of Terrain on Climate." *Global Change Biology* 17 (2): 1022–35. <https://doi.org/10.1111/j.1365-2486.2010.02263.x>.
- Dyer, James M. 2019. "A GIS-Based Water Balance Approach Using a LiDAR-Derived DEM Captures Fine-Scale Vegetation Patterns." *Remote Sensing* 11 (20, 20): 2385. <https://doi.org/10.3390/rs11202385>.
- Laufenberg, David, David Thoma, Andrew Hansen, and Jia Hu. 2020. "Biophysical Gradients and Performance of Whitebark Pine Plantings in the Greater Yellowstone Ecosystem." *Forests* 11 (1, 1): 119. <https://doi.org/10.3390/f11010119>.
- Lawrence, David J., Amber N. Runyon, John E. Gross, Gregor W. Schuurman, and Brian W. Miller. 2021. "Divergent, Plausible, and Relevant Climate Futures for near- and Long-Term Resource Planning." *Climatic Change* 167 (3): 38. <https://doi.org/10.1007/s10584-021-03169-y>.
- Lin, Yuh-Lang, Sen Chiao, Ting-An Wang, Michael L. Kaplan, and Ronald P. Weglarz. 2001. "Some Common Ingredients for Heavy Orographic Rainfall." *Weather and Forecasting* 16 (6): 633–60. [https://doi.org/10.1175/1520-0434\(2001\)016<0633:SCIFHO>2.0.CO;2](https://doi.org/10.1175/1520-0434(2001)016<0633:SCIFHO>2.0.CO;2).
- Stephenson, Nathan. 1998. "Actual Evapotranspiration and Deficit: Biologically Meaningful Correlates of Vegetation Distribution across Spatial Scales." *Journal of Biogeography* 25 (5): 855–70. <https://doi.org/10.1046/j.1365-2699.1998.00233.x>.
- Tercek, Michael T., John E. Gross, and David P. Thoma. 2023. "Robust Projections and Consequences of an Expanding Bimodal Growing Season in the Western United States." *Ecosphere* 14 (5): e4530. <https://doi.org/10.1002/ecs2.4530>.
- Tercek, Michael T., David Thoma, John E. Gross, Kirk Sherrill, Stefanie Kagone, and Gabriel Senay. 2021. "Historical Changes in Plant Water Use and Need in the Continental United States." *Plos One* 16 (9): e0256586. <https://doi.org/10.1371/journal.pone.0256586>.